Thermodynamic Behavior of Reactive Azeotropes

Matthew J. Okasinski and Michael F. Doherty
Dept. of Chemical Engineering, University of Massachusetts, Amherst, MA 01003

During process design of reactive distillation systems, there is often uncertainty in the value of the reaction equilibrium constant (K_{eq}), whether it is determined experimentally or calculated from thermochemical data. The effect of the reaction equilibrium constant on the existence and location of reactive azeotropes (constant boiling reactive mixtures) is explored for chemical equilibrium systems with a single chemical reaction. With a known set of starting points, arc-length continuation was used to track solutions of the equations for reactive azeotropy as a function of the reaction equilibrium constant. The results, portrayed in bifurcation diagrams, reveal that azeotropes may appear or disappear as the equilibrium constant is varied. Results for the esterification of acetic acid with ethanol indicate three distinct regions of phase behavior. The first regime ($K_{eq} < 0.449$) contains a quaternary saddle reactive azeotrope. At intermediate values of the reaction equilibrium constant ($0.449 < K_{eq} < 12.5$), there are no reactive azeotropes in the system. In the third regime ($K_{eq} > 12.5$), a minimum-boiling quaternary reactive azeotrope appears. In addition, for three reported literature values of the reaction equilibrium constant, each one lies in a different regime. Other examples also illustrate the broad taxonomy of reactive azeotropic systems.

Introduction

The existence and importance of azeotropes in ordinary distillation has been widely studied for many years. Azeotropes alter product distributions and attainable regions; cause distillation boundaries to occur; and have led to the creation of extractive and azeotropic distillation technology. Within the last decade, reactive distillation has become increasingly attractive as a potential process alternative for simultaneously conducting liquid-phase reaction and vapor–liquid separation. It can be expected that reactive azeotropes have a similar impact on reactive distillation, as Espinosa et al. (1995) noted in their work determining reactive-distillation product-composition regions in mixtures containing reactive azeotropes. In contrast to nonreactive azeotropes, however, very little is known about reactive azeotropes; especially their behavior as thermodynamic parameters are varied. For example, during process design and development, there are often uncertainties in the value of the reaction equilibrium constant. It is important to know how sensitive the phase behavior is to these uncertainties.

Reaction equilibrium constants are calculated from either Gibbs free energies of formation or from experimental equilibrium composition measurements. Different researchers studying the same chemical system often arrive at different values of the reaction equilibrium constant. For example, Columbo et al. (1983) and Rehfinger and Hoffmann (1990) have different expressions (leading to different values) for the reaction equilibrium constant for the synthesis of methyl *tert*-butyl ether (MTBE) over the same temperature range. Similarly, Smith and Van Ness (1975), Dean (1979), and Kang et al. (1992) predict different reaction equilibrium constants for the esterification of acetic acid with ethanol. Barbosa and Doherty (1988b) illustrated the effect that changes in the reaction equilibrium constant have on residue curve maps for this system, noting the appearance and disappearance of a quaternary reactive azeotrope.

There exists a small experimental database for chemical systems in both phase and reaction equilibrium. The formaldehyde–water system, which contains multiple reactions, has been studied extensively [e.g., Gmehling and Onken (1977), Brandani et al. (1980), Maurer (1986), and Albert et al. (1996)]. Albert et al. (1996) also examined the reactive system of formaldehyde and methanol. Esterification reaction systems have also been studied. For example, Rhim et al. (1985) examined the formic acid–ethanol–water–ethyl for-

Correspondence concerning this article should be addressed to M. F. Doherty.

mate system; Kang et al. (1992) reported phase and reaction equilibrium data for the system of acetic acid–ethanol–water–ethyl acetate; and Lee and Kuo (1996) also reported phase and reaction equilibrium data for the mixture of acetic acid–isopropanol–water–isopropyl acetate.

Barbosa and Doherty (1987) derived the necessary and sufficient conditions for reactive azeotropy in systems with a single chemical reaction. Ung and Doherty (1995b) extended these conditions to multiple reaction systems. These equations provide the basis for the equation set analyzed in this article. They also determined when a nonreactive azeotrope will survive the reaction, a result that lends insight into the phase behavior of reactive systems.

In recent years, arc-length continuation has been used successfully to track fixed-point branches of nonlinear algebraic equations using a variety of parameters. One of the pioneers of this technique in chemical engineering was Seader and coworkers, who used arc-length continuation to solve for all the real solutions to an interlinked distillation system using a global homotopy parameter (Lin et al., 1987). Fidkowski et al. (1993) used a homotopy parameter to calculate the temperature and composition of all azeotropes in a nonreactive multicomponent mixture. Venimadhavan et al. (1994, 1995) examined the location of fixed points for the simple reactive distillation system of MTBE as the Damkohler number was varied. In this article, reactive azeotrope branches are reported as a function of the reaction equilibrium constant (K_{eq}), using arc-length continuation. The results provide quantitative sensitivity of the phase behavior to uncertainties in the value of K_{eq}. In addition, K_{eq} can be adjusted through changes in system pressure, which influences the boiling point of the mixture (and hence K_{eq}). It is useful, therefore, to know the location of the reactive azeotropes over a range of values of K_{eq}, since a change in pressure may alter the structure of the phase diagram in such a way as to influence the feasibility of the desired reaction–separation.

Thermodynamics

Equation set

Ung and Doherty (1995a) introduced a set of transformed composition variables whose values remain constant during reaction and that sum to unity. These transformed variables also reduce the dimensionality of the problem by one, as required by the phase rule, so that a ternary reactive system can be represented in the same way as a binary nonreactive system. For these reasons, it is convenient to view reactive systems in terms of these transformed composition variables. Ung and Doherty (1995b) give the necessary and sufficient conditions for reactive azeotropes to exist, defined in terms of these transformed composition variables. For a single chemical reaction, an azeotrope occurs in a reactive mixture when

$$Y_i - X_i = 0 \qquad i = 1, \ldots, C-2 \tag{1}$$

where

$$X_i \equiv \left(\frac{\nu_k x_i - \nu_i x_k}{\nu_k - \nu_T x_k} \right) \qquad Y_i \equiv \left(\frac{\nu_k y_i - \nu_i y_k}{\nu_k - \nu_T y_k} \right).$$

The subscript k signifies the reference component as defined by Ung and Doherty (1995a). The liquid and vapor mole fractions are related by phase and reaction equilibrium. Ung and Doherty (1995b) proved that pure components and nonreactive azeotropes surviving the reaction also satisfy Eq. 1.

Equation 2 is the thermodynamic definition of the reaction equilibrium constant where, by convention, the stoichiometric coefficients are negative for reactants and positive for products:

$$K_{eq} = \prod_{i=1}^{c} a_i^{\nu_i}. \tag{2}$$

Equation 2 is ill-conditioned as K_{eq} approaches infinity. A better formulation of the reaction equilibrium equation is obtained by dividing Eq. 2 by $(K_{eq}+1)$ and rearranging to yield Eq. 3:

$$\left(\frac{K_{eq}}{K_{eq}+1} \right) \prod a_{react}^{|\nu_{react}|} - \left(\frac{1}{K_{eq}+1} \right) \prod a_{prod}^{|\nu_{prod}|} = 0. \tag{3}$$

The variables a_{react} and a_{prod} are the activities of the reactants and products, respectively. They are defined as $a_i \equiv x_i \gamma_i$, where γ is the activity coefficient determined by a nonideal solution model. Equations 1 and 3, along with the phase equilibrium relationship, form the equation set to be solved by arc-length continuation, using the software package AUTO (Doedel, 1986). The advantage of arc-length continuation over other techniques is that the branches are parameterized in arc length, which makes the method robust around turning points and at bifurcations (intersecting branches) (Keller, 1977; Seydel, 1994).

Starting points

Equation 3 leads to the development of a complete set of starting points for the arc-length continuation technique. This equation is satisfied and simplifies to Eq. 4a in the limit as K_{eq} approaches zero (complete back reaction). The first set of starting points is all pure components and nonreactive azeotropes that satisfy Eq. 4a:

$$\text{As} \quad K_{eq} \to 0,$$
$$\prod a_{prod}^{|\nu_{prod}|} = 0. \tag{4a}$$

Similarly, in the limit as K_{eq} approaches infinity (complete forward reaction), Eq. 3 is satisfied and simplifies to Eq. 4b. The second set of starting points is all pure components and nonreactive azeotropes that satisfy Eq. 4b:

$$\text{As} \quad K_{eq} \to \infty,$$
$$\prod a_{react}^{|\nu_{react}|} = 0. \tag{4b}$$

Both sets of starting points must be used to completely track all the reactive azeotrope branches in the system, assuming that no isola exist. However, after forming the sets of starting points by inspection, each set must be checked for degenerate solutions that disappear immediately (i.e., are not a solu-

tion) as parameters are changed. These degenerate solutions to Eq. 4a or 4b do not correspond to a starting point of a branch, and therefore must be discarded before beginning the continuation technique.

Transforming the reactive phase diagram in mole fraction coordinates into the equivalent diagram in transformed composition variables derived in Ung and Doherty (1995a), allows for an intuitive, qualitative understanding of reactive azeotropic behavior and for the detection of degenerate solutions to the starting-point equations. For a ternary reactive system, the mole fraction triangle collapses to a line (a reactive edge), as shown in Figure 1b. In transformed composition variable coordinates, two components that can react are connected by a reactive edge. In Figure 1b, components B and C are connected by a reactive edge, since mixtures of components B and C are able to form component A. Any point on this edge represents an equilibrium mixture of all three components. A nonreactive edge, which connects two components that do not react, is seen in the last example. For quaternary reactive systems, the mole-fraction space is tetrahedral and becomes planar in transformed composition variable coordinates, as seen in Example 5.

Branches of reactive azeotropes may arise from starting points (pure components or nonreactive azeotropes) that are nondegenerate solutions of Eq. 4a or 4b. Nondegenerate solutions (node or saddle) of Eq. 4a or 4b are regular points (i.e., not bifurcation points) and give rise to a single branch of solutions as K_{eq} varies. Degenerate solutions of Eq. 4a or 4b are typically saddle-node bifurcation points, and give rise to either multiple branches or no branch of solutions. Continuation techniques cannot be started at bifurcation points. However, this does not present a problem for the method described in this article, since alternate starting points exist

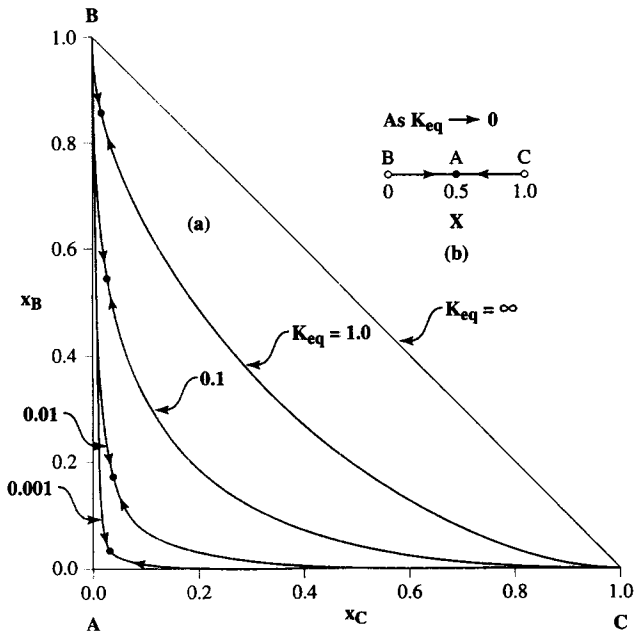

Figure 1. Reactive phase diagrams for the decomposition reaction $2A \rightleftharpoons B + C$ at various values of K_{eq}.

The solid circles signify the position of a reactive azeotrope; the arrows point in the direction of increasing boiling temperature.

that can detect these bifurcations if they exhibit multiple branches. This article also shows that azeotropes that possess nondegenerate stabilities will become reactive azeotropes. Whether a reactive azeotrope persists for all values of K_{eq} can only be determined by branch tracking. Nonreactive azeotropes that lie on nonreactive edges will survive the reaction and remain a nonreactive azeotrope for all values of the reaction equilibrium constant (Ung and Doherty, 1995b).

For ternary systems, degenerate solutions of Eqs. 4a and 4b appear as inflexion singular points on phase diagrams in transformed composition variables. For quaternary systems, degenerate solutions of the starting point equations correspond to starting points that possess a saddle-node stability. Both inflexion singular points and saddle nodes possess a degenerate stability, that is to say, a slight change in the parameter will cause these structures to disappear. These findings are further illustrated in the second and last examples of this article for ternary and quaternary systems, respectively.

Noting that finding all azeotropes in a general nonreactive multicomponent mixture is difficult, Fidkowski et al. (1993) found that binary azeotropes arise as bifurcations from pure component branches, and ternary azeotropes as bifurcations from binary azeotrope branches, and so on. Likewise, reactive azeotropes can be tracked from selected nonreactive azeotropes and pure components (i.e., nondegenerate solutions of Eq. 4a or 4b), thereby applying the extensive database available on nonreactive azeotropic mixtures to determining the starting points for this branch tracking method. The solutions of Eqs. 1 and 3, together with a phase-equilibrium relation, are tracked using arc-length continuation with the reaction equilibrium constant as the continuation parameter and starting points obtained from the known nondegenerate solutions of Eqs. 4a and 4b. For scaling purposes, the continuation parameter is defined as $K_{eq}/(K_{eq}+1)$.

The results of the continuation technique are displayed on a bifurcation diagram, which plots a characteristic feature of the solution vector (e.g., norm) vs. the continuation parameter. As in Fidkowski et al. (1993), the equilibrium temperature is chosen instead of the norm, since it is independent of problem dimensionality and indicates whether a given reactive azeotrope is minimum boiling, maximum boiling, or intermediate boiling. The use of both reactive phase diagrams and bifurcation diagrams is illustrated in the next section.

Examples and Discussion

Five examples were chosen to demonstrate the wide taxonomy of reactive azeotropes. In the first example, a reactive azeotrope appears in a system that contains no azeotropes of any kind before reaction. Barbosa and Doherty (1988a) proved that this situation could exist even in systems exhibiting constant relative volatility. The second example illustrates a ternary system with a degenerate solution to the starting-point equations. In each of the next two examples, reactive azeotropes arise from both a pure component vertex and a nonreactive binary azeotrope. These two reactive azeotropes are shown to approach each other and both are eliminated by a turning-point bifurcation as the reaction equilibrium constant is changed. The final example is the esterification of acetic acid with ethanol; a four-component system that contains a ternary nonreactive azeotrope and binary azeotropes on both reactive and nonreactive edges.

Table 1. Thermodynamic Data for Example 1

Component	A	B	C
Normal boil. pt. (K)	339.60	310.08	276.87
Antoine coeff.			
A_1	20.7312	20.723	20.6909
A_2	−2,680.52	−2,462.02	−2,202.188
A_3	−48.401	−42.391	−36.578

Example 1

The first example is an equilibrium decomposition reaction of the form $2A \Leftrightarrow B + C$, where A is the highest boiling component and C is the lowest boiling component. The system pressure is atmospheric, Raoult's law was assumed for vapor–liquid equilibrium, and thermodynamic properties are listed in Table 1. Figure 1a shows reaction equilibrium curves for various values of K_{eq}. Notice that as the reaction equilibrium constant approaches zero, the curves lie alongside the A-B and A-C edges. As K_{eq} asymptotically approaches zero, a maximum-boiling reactive azeotrope appears near the pure A vertex. Figure 1a also shows where this reactive azeotrope moves as K_{eq} is increased. As K_{eq} approaches infinity, the reactive azeotrope merges with a pure-product vertex because there are no nonreactive azeotropes on the B-C edge and Eq. 4b must be satisfied in its limit.

Choosing component A as the reference component and transforming the reactive diagram in mole-fraction coordinates, using the method developed by Ung and Doherty (1995a), the triangular diagram is reduced to a reactive edge, shown in Figure 1b, where in the limit as K_{eq} approaches zero, the reactant (A) is a stable node in the system. As was shown in Figure 1a, a reactive azeotrope emerges from this node. The movement of this reactive azeotrope as K_{eq} is varied also appears on Y-X diagrams, shown in Figure 2. As K_{eq} asymptotically approaches zero, the reactive azeotrope approaches the pure component A vertex, which lies at a transformed liquid composition value of 0.5 (this value only satisfies Eq. 3 in the limit as K_{eq} approaches zero). As K_{eq} increases, the reactive azeotrope moves toward $X = 0$, which is pure component B. Pure components B and C satisfy Eqs. 1 and 3 at all values of K_{eq}, forming their own separate branches of solutions in the bifurcation diagram shown in Figure 3. The diagram also reveals a maximum-boiling reactive azeotrope emerging from the pure A vertex in the limit of complete back reaction ($\lim K_{eq} \to 0$) and traveling through the composition diagram, merging with pure component B in the limit of complete forward reaction ($\lim K_{eq} \to \infty$).

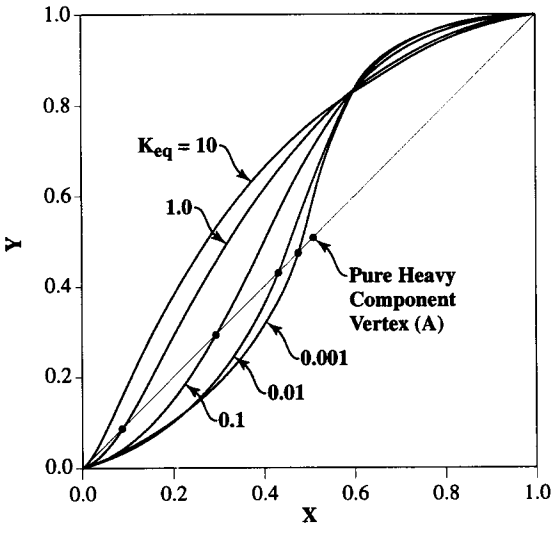

Figure 2. Y-X diagrams for the decomposition reaction, $2A \rightleftharpoons B + C$ at various values of K_{eq}.

The solid circles signify the position of a reactive azeotrope.

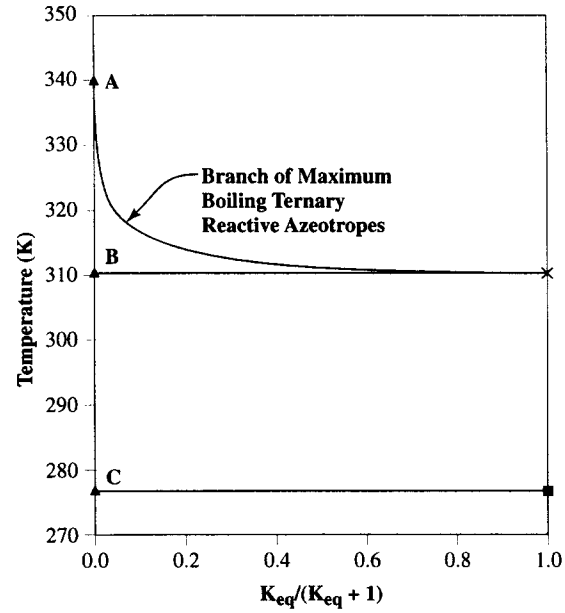

Figure 3. Bifurcation diagram for the decomposition reaction in Example 1.

Triangles and squares signify valid starting points, × signifies a degenerate solution of Eq. 4b and is not used as a starting point.

Example 2

Consider again an equilibrium reaction of the form $2A \Leftrightarrow B + C$, where B and C are the highest and lowest boiling components, respectively, and a maximum-boiling azeotrope occurs between component A and component B in the nonreactive mixture (see Figure 4a). We assume the system is isobaric at 1 atm pressure, the vapor–liquid equilibrium relationship is given by Eq. A1 in the Appendix and the thermodynamic properties are listed in Table 2. Again, choosing component A as the reference component and transforming

Table 2. Thermodynamic Data for Example 2

Component	A	B	C
Normal boil. pt. (K)	388.35	454.95	329.21
Antoine coeff.			
A_1	21.1056	20.85085	21.3099
A_2	−3,163.289	−3,183.67	−2,801.53
A_3	−58.171	−113.657	−42.875
Wilson coeff. (cal/mol)			
A	—	−1,199.743	−294.815
B	−548.092	—	3,103.52
C	855.756	−819.897	—
Molar vol. (mL/mol)	80.86	83.14	74.05

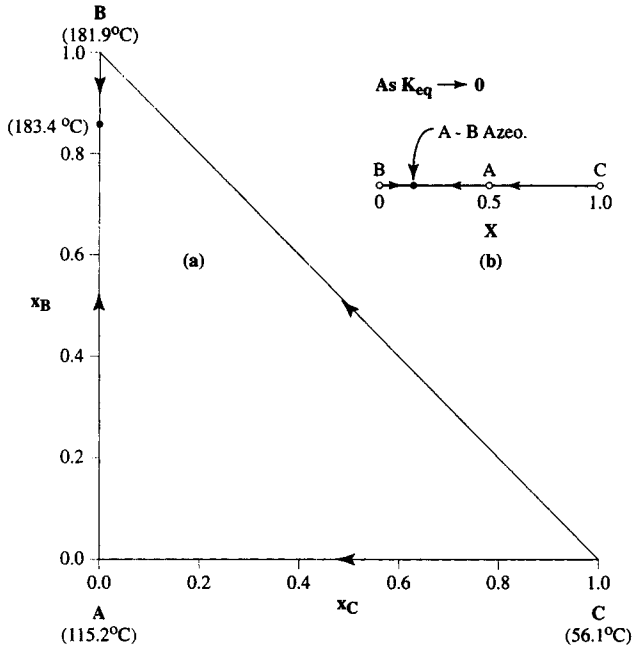

Figure 4. Example 2: (a) residue curve map for the nonreactive mixture; (b) equilibrium reactive phase diagram in the transformed composition variable as $K_{eq} \rightarrow 0$.

the diagram in mole fraction coordinates into a reactive phase diagram in transformed composition variables, the starting points are obtained by inspection of Eqs. 4a and 4b, in their respective limits. From this diagram, shown in Figure 4b, it is seen that pure component A is neither a local maximum nor minimum in temperature, but is an inflexion singular point that by its nature possesses a degenerate stability. Therefore, it is a degenerate starting point and must be discarded from the set of starting points for the continuation technique. At least three branches of solutions are expected based on the number of nondegenerate starting points (namely, pure B, pure C, and the A-B azeotrope for $K_{eq} \rightarrow 0$, and pure B and pure C for $K_{eq} \rightarrow \infty$). In Figure 5, a bifurcation diagram shows that as K_{eq} increases, the maximum-boiling azeotrope moves into the composition triangle, becoming a ternary reactive azeotrope. As K_{eq} continues to increase, this reactive azeotrope moves toward the B vertex, merging with it in the limit of complete forward reaction. Pure components B and C are solutions to Eqs. 1 and 3 for all values of K_{eq} and have their own branches in Figure 5.

Example 3

The third example is a ternary system that exhibits a minimum-boiling azeotrope on the A-B edge of the triangular diagram, causing a distillation boundary to occur in the nonreactive mixture. The residue curve map for the nonreactive mixture is shown in Figure 6a. We assume the system is isobaric at 1-atm pressure, the vapor–liquid equilibrium is represented by Eq. A1 in the Appendix and the thermodynamic properties are listed in Table 3. We again consider a reaction of the form $2A \Leftrightarrow B + C$, where B is the highest boiling component and C is the lowest boiling component. In this example it is not as easy to anticipate the existence or non-

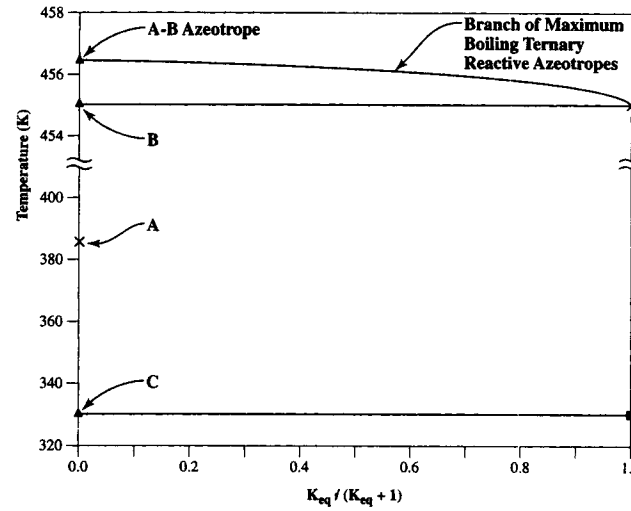

Figure 5. Bifurcation diagram for Example 2.

The solid triangles and squares signify valid starting points and × signifies a degenerate solution of either Eq. 4a or 4b and is not used as a starting point.

existence of reactive azeotropes as it was with the previous examples, due to the more complex nature of the underlying phase equilibrium. Choosing component A as the reference component and transforming the reactive diagram in mole-fraction coordinates reveals a reactive edge where, as K_{eq} asymptotically approaches zero, both the nonreactive azeotrope and the reactant (A) are nodes, as shown in Figure 6b. It is expected that a reactive azeotrope will arise from each of these singular points as K_{eq} is increased, and this is confirmed in the Y-X and T-Y, X diagrams shown in Figures 7 and 8, respectively. Figure 9 shows a bifurcation diagram

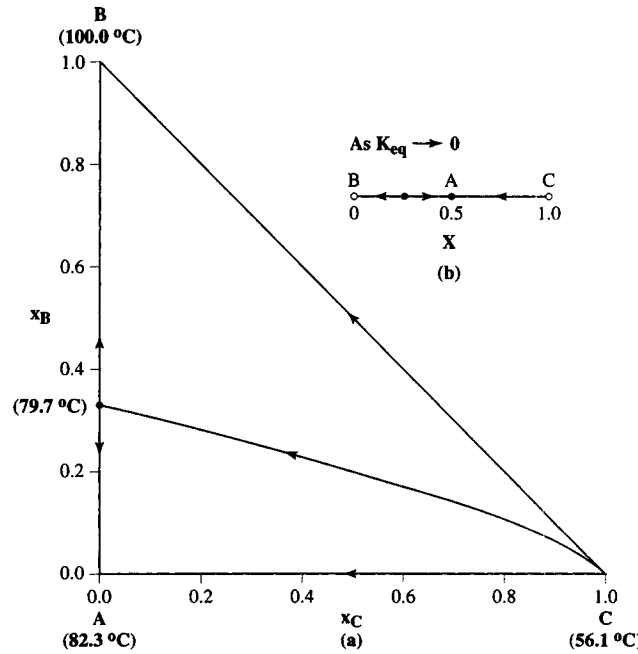

Figure 6. Example 3: (a) residue curve map for the nonreactive mixture; (b) equilibrium reactive phase diagram in the transformed composition variable as $K_{eq} \rightarrow 0$.

Table 3. Thermodynamic Data for Example 3

Component	*A*	*B*	*C*
Normal boil. pt. (K)	355.49	373.15	329.21
Antoine coeff.			
A_1	21.536	23.2256	21.3099
A_2	−2,545.64	−3,835.18	−2,801.53
A_3	−101.183	−45.343	−42.875
Wilson coeff. (cal/mol)			
A	—	1,587.7271	1.0
B	1,380.3987	—	1,448.0099
C	1.0	291.27080	—
Molar vol. (mL/mol)	94.88	18.07	74.04

for the system illustrating that at very low K_{eq} (~ 0.027) these two reactive azeotropes meet and eliminate each other in a turning-point bifurcation. At this value of K_{eq}, the distillation boundary vanishes. However, these azeotropes leave behind a strong tangent pinch that gradually weakens as K_{eq} is increased, as seen in Figure 7.

These bifurcation and reactive phase diagrams are useful for process design and development. There are many reactions that exhibit the type of phase behavior shown in the first three examples. Some reaction separations will be accomplished more easily than others, based solely on the value of the thermodynamic reaction equilibrium constant. In the first example, the temperatures of the ternary reactive azeotrope and the component *B* are indistinguishable above a reaction equilibrium constant of about 5.0 (the reactive azeotrope merges with pure *B*), allowing for the possibility of obtaining high-purity decomposition products at a relatively low reaction equilibrium constant using reactive distillation. The results from the present example show that at very low K_{eq}, the proposed reaction separation will be inhibited by the presence of two reactive azeotropes. At higher values of K_{eq}, the two reactive azeotropes disappear, and both products (*B* and *C*) are feasible in high purity. However, the presence of a tangent pinch may complicate the process design. Changing the system pressure may adjust the reaction equilibrium constant enough to alleviate the tangent pinch.

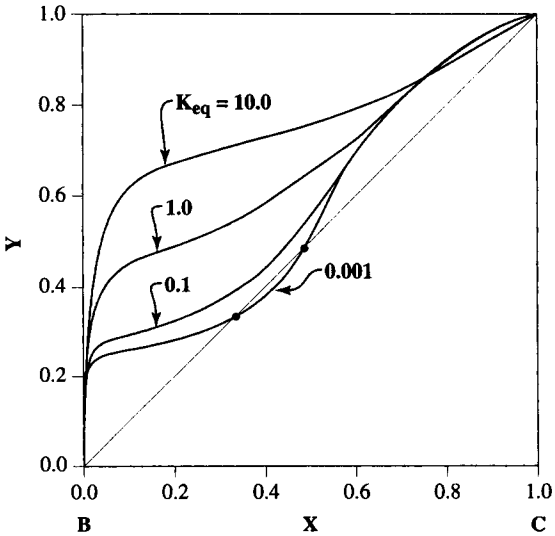

Figure 7. *Y-X* diagram for Example 3 at various values of K_{eq}.
The solid circles signify the position of a reactive azeotrope.

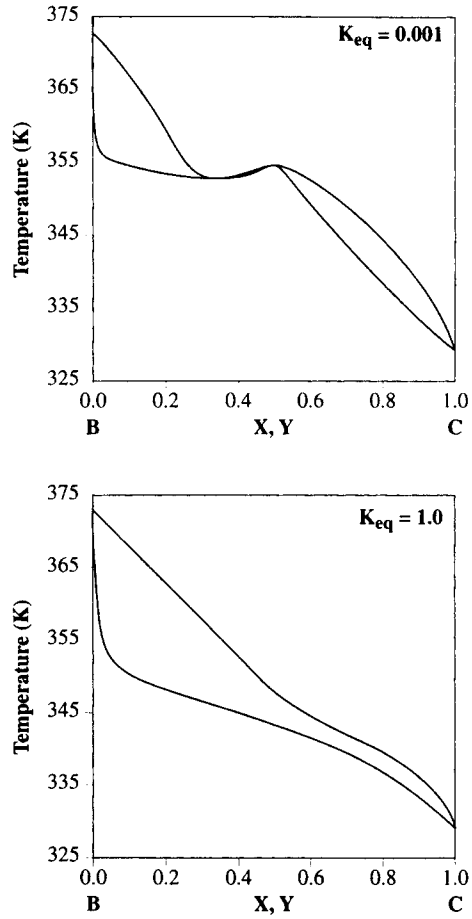

Figure 8. *T-Y, X* diagrams for Example 3 at different values of K_{eq}.

Example 4

The fourth example is the isobutene (i-C_4)–methanol (MeOH)–methyl *tert*-butyl ether (MTBE) system that exhibits two minimum-boiling azeotropes at 8 atm. The equilibrium reaction is MeOH + Isobutene ⇔ MTBE, the reference component is MTBE and the thermodynamic properties are listed in Table 4. The nonreactive residue curve map in

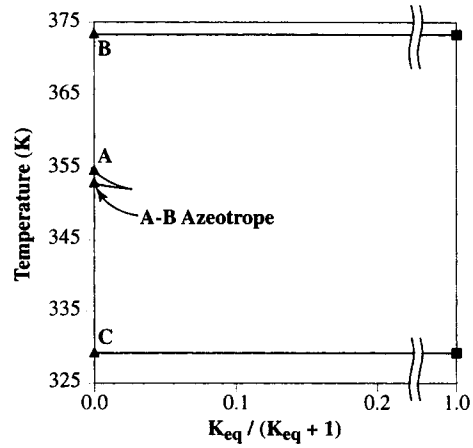

Figure 9. Bifurcation diagram for Example 3.
The solid triangles and squares signify valid starting points.

Table 4. Thermodynamic Data for Example 4

Component	Isobutene	Methanol	MTBE
Normal boil. pt. (K)	266.2607	337.69	328.229
Antoine coeff.			
A_1	20.6455	23.4832	20.71616
A_2	−2,125.7489	−3,634.01	−2,571.5846
A_3	−33.16	−33.768	−48.406
Wilson coeff. (cal/mol)			
i = Isobutene	—	169.9953	−60.1022
i = Methanol	2576.8532	—	1,483.2478
i = MTBE	271.5669	−406.3902	—
Molar vol. (mL/mol)	93.33	44.44	118.8

mole-fraction coordinates and the reactive phase diagrams in transformed composition variable coordinates are shown in Figure 10. One nonreactive azeotrope lies on the isobutene–methanol edge, the other lies on the methanol–MTBE edge with a distillation boundary connecting the two azeotropes (Figure 10a). The two reactive phase diagrams, one in the limit as K_{eq} approaches zero and the other as K_{eq} approaches infinity, reveal that both nonreactive azeotropes and the pure MTBE vertex are nodes lying on a reactive edge. Each of these nodes, which have nondegenerate stabilities, correspond to valid starting points and each will yield a branch of reactive azeotropes. Therefore, at least three reactive azeotropes are expected in this system. Whether all three reactive azeotropes will appear simultaneously at a given value of K_{eq} cannot be known *a priori*, since one node exists in the limit of complete back reaction and the other two nodes exist in the limit of complete forward reaction.

The bifurcation diagram, shown in Figure 11a, reveals the presence of three reactive azeotropes. The first reactive azeotrope emerges at low K_{eq} from the binary nonreactive

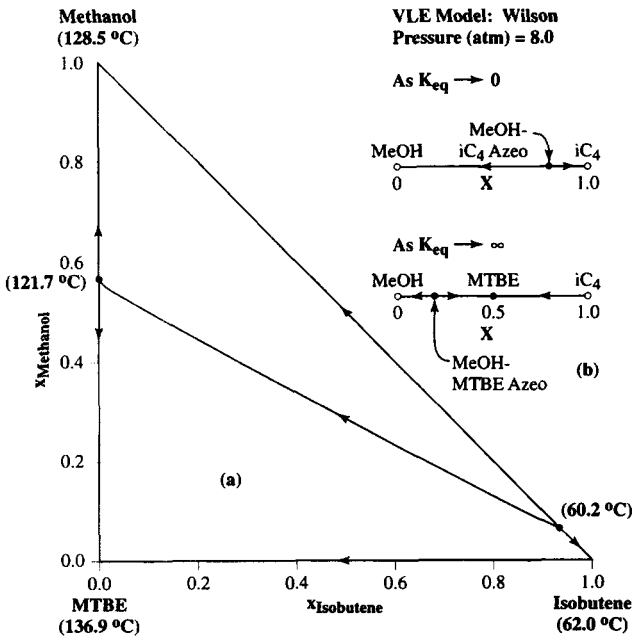

Figure 10. Phase diagram for isobutene–methanol–MTBE system at 8 atm.

(a) Residue curve map for the nonreactive mixture; (b) equilibrium reactive phase diagrams in transformed composition variable as $K_{eq} \rightarrow 0$ and as $K_{eq} \rightarrow \infty$.

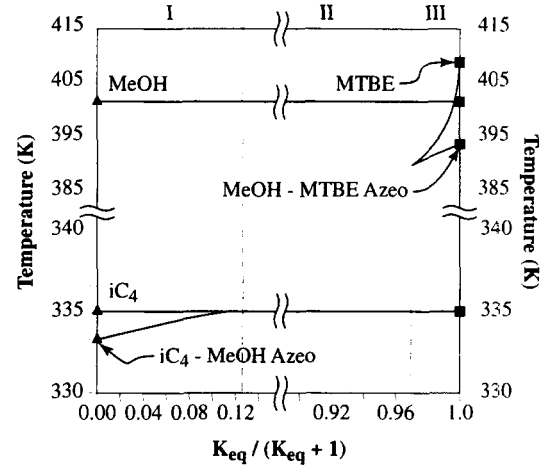

Figure 11a. Bifurcation diagram for the isobutene–methanol– MTBE system at 8 atm (the solid triangles and squares signify valid starting points).

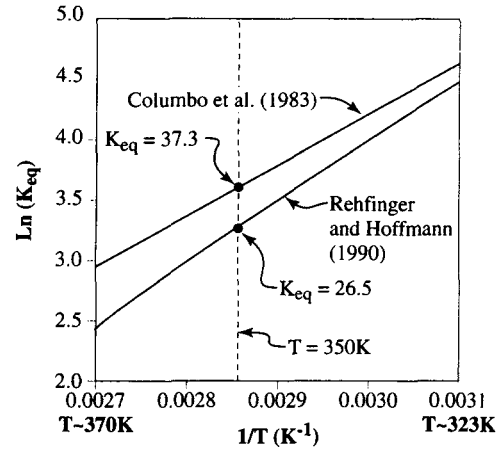

Figure 11b. Two K_{eq} correlations for the MTBE chemistry.

isobutene–methanol azeotrope and quickly merges into the pure isobutene vertex. The other two reactive azeotropes emerge from the pure MTBE vertex and the nonreactive methanol–MTBE azeotrope in the limit of complete forward reaction. There is a limit point at $K_{eq} \cong 31.9$ where these two reactive azeotropes eliminate each other at a turning-point bifurcation and the distillation boundary disappears. In this example, both sets of starting points (Eqs. 4a and 4b) are needed to completely calculate the solution branches for this system.

Figure 11a also shows the three fundamental changes that the residue curve maps for the MTBE system will undergo as the reaction equilibrium constant changes, and Figure 12 illustrates a typical phase diagram for each region. In the first region, $K_{eq} < 0.145$, a ternary reactive azeotrope emerges from the isobutene–methanol azeotrope and merges with the pure isobutene vertex. Figure 12a shows the presence of a reactive azeotrope near the pure isobutene vertex ($X = 1.0$) for $K_{eq} = 0.04$. In the second region, $0.145 < K_{eq} < 31.9$, there are no azeotropes of any kind in the system. Figure 12b re-

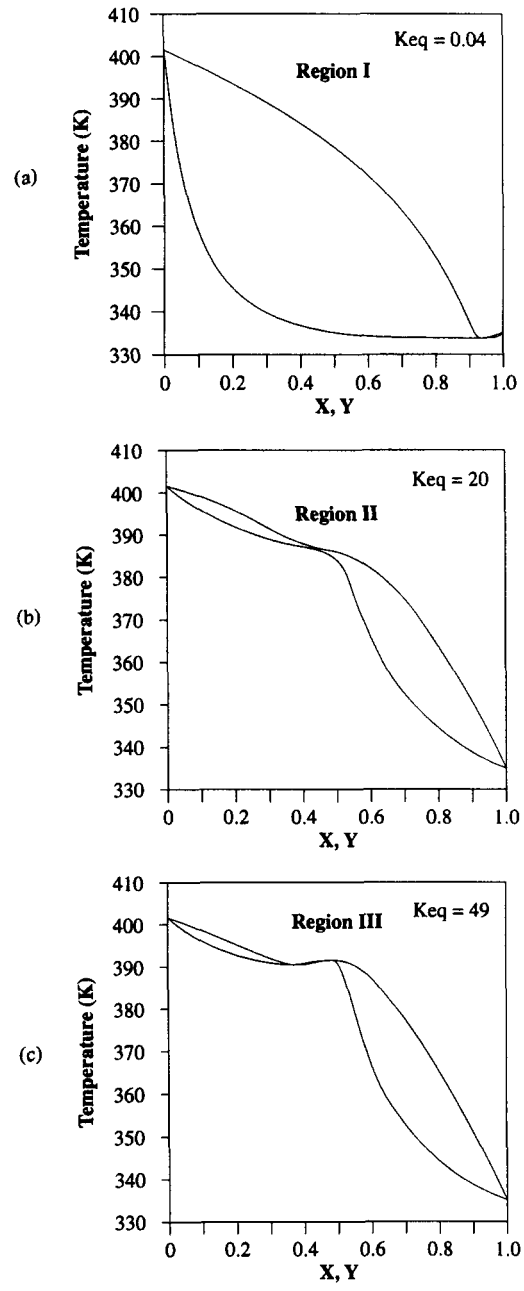

Figure 12. Typical *T-X, Y* diagrams for each region of the MTBE system.

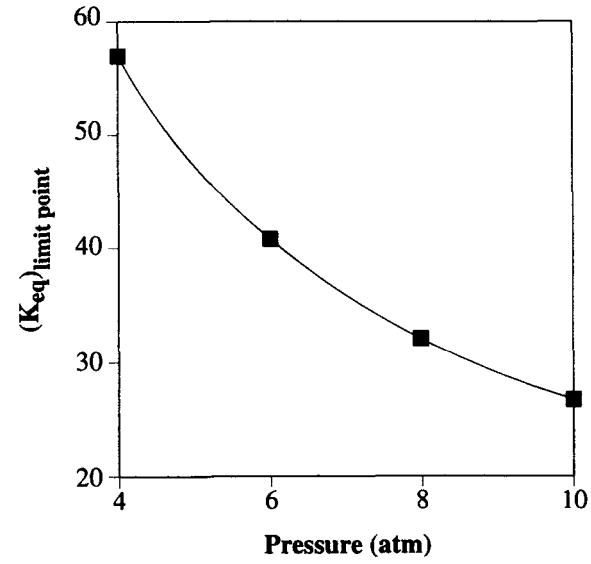

Figure 13. Reaction equilibrium constant at the limit point as a function of pressure.

veals a severe tangent pinch, but no azeotrope for $K_{eq} = 20$. The severity of the tangent pinch will increase as K_{eq} increases toward the limit point. At the limit point ($K_{eq} \cong 31.9$), two reactive azeotropes appear at the same point, which divide and separate as K_{eq} is increased. In the third region ($K_{eq} > 31.9$), there are two reactive azeotropes in the system, one of which is in the vicinity of the pure MTBE vertex. In contrast to the previous examples, the reactive azeotrope near the pure MTBE vertex is beneficial because it causes high-purity MTBE to be obtained as a product from a reactive distillation column (Ung and Doherty, 1995a). For $K_{eq} = 49$, Figure 12c illustrates the presence of two reactive azeotropes, one of which is near the pure MTBE vertex ($X = 0.5$).

The reaction equilibrium constants chosen for Figures 12b and 12c lie on either side of the limit point. Both of these values are within the range reported by Columbo et al. (1983) and Rehfinger and Hoffmann (1990), who reported different values for the reaction equilibrium constant over the same temperature range (see Figure 11b). At 350 K, Columbo et al. (1983) reported a value of 37.3, while Rehfinger and Hoffmann (1990) reported a value of 26.5. As seen from the bifurcation diagram (Figure 11a), these values are in regions exhibiting different phase behavior.

Noting that decreasing the column pressure increases the reaction equilibrium constant, moving the chemical equilibrium curve closer to the MTBE vertex, Venimadhavan et al. (1994, 1995) proposed that a continuous column operating at lower pressures may yield MTBE at higher purities. Figure 13 shows the movement of the limit point as the system pressure is changed. Note that as the pressure is decreased, the limit point moves in a favorable direction toward greater forward reaction. Since larger equilibrium constants are preferred, then from a thermodynamic point of view, lower operating pressures are advantageous.

Example 5

The final example is the esterification of acetic acid (AA) with ethanol (EtOH) to form ethyl acetate (EA) and water (W). The equilibrium reaction is shown below:

$$\text{Acetic Acid} + \text{Ethanol} \Leftrightarrow \text{Ethyl Acetate} + \text{Water}.$$

We assume the system is isobaric at atmospheric pressure, the vapor–liquid equilibrium relationship is given in Eq. A2 of the Appendix and the thermodynamic properties, from Barbosa and Doherty (1988a), are given in Table 5. The nonreactive quaternary system exhibits three minimum-boiling binary azeotropes (EtOH–W, EtOH–EA, EA–W) and a minimum-boiling ternary azeotrope (EA–W–EtOH).

Table 5. Thermodynamic Data for Example 5

Component	Ethyl Acetate	Ethanol	Water	Acetic Acid
Normal boil. pt. (K)	350.21	351.44	373.15	391.01
Antoine coeff.				
A_1	21.245216	23.571771	23.477618	21.903824
A_2	−2,866.6056	−3,667.7049	−3,984.9228	−3,530.5836
A_3	−55.279	−46.976	−39.734	−50.851
Dimerization const.				
D_1	—	—	—	−12.5454
D_2	—	—	—	3,166.0
Wilson coeff. (cal/mol)				
Ethyl acetate	—	57.3883	53,616.9256	−922.3772
Ethanol	572.7132	—	393.8147	202.0164
Water	2,376.035	926.246	—	801.1524
Acetic acid	3,477.469	−259.6331	4.0362	—
Molar vol. (mL/mol)	98.49	58.69	18.07	57.54

As K_{eq} approaches infinity (complete forward reaction), the equilibrium surface, shown in Figure 14a, is asymptotically close to the EA–W–AA and EA–W–EtOH faces of the tetrahedron. This is easy to anticipate because the components present at the complete forward reaction must be EA and W, in addition to any unreacted AA or unreacted EtOH. The starting points on these faces satisfy Eq. 4b. Likewise as K_{eq} approaches zero (complete back reaction), the equilibrium surface, shown in Figure 14b, is asymptotically close to the EtOH–AA–W and EtOH–AA–EA faces of the tetrahedron. By analogy with the complete forward reaction case, the reaction equilibrium surface will lie on the faces of the composition space that contain both reactants and one of the products. The starting points for the limit of complete back reaction satisfy Eq. 4a. At intermediate values of K_{eq}, the reaction equilibrium surface lies within the composition tetrahedron.

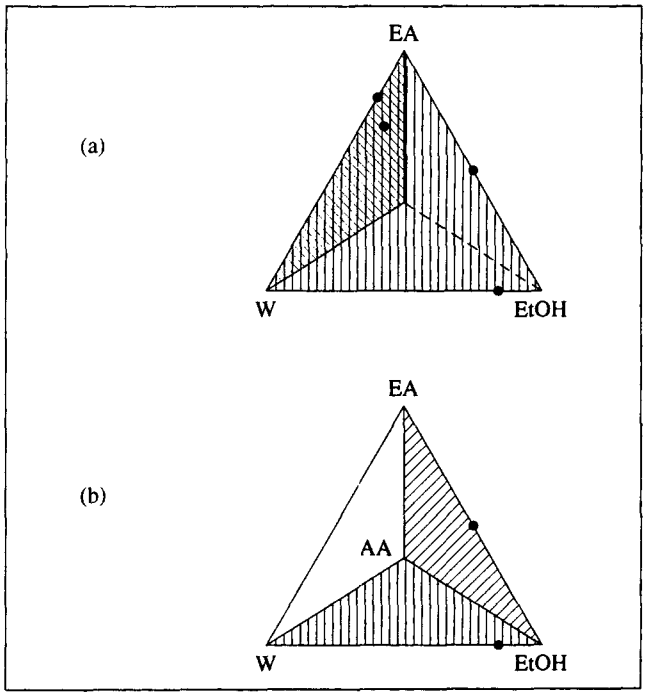

Figure 14. Reactive equilibrium surfaces (a) as K_{eq} approaches ∞, and (b) as K_{eq} approaches 0.

The solid circles signify the location of azeotropes and the dashed line represents a hidden edge.

Several researchers have studied this system and there is a substantial amount of uncertainty in the value of the reaction equilibrium constant. The values reported by Smith and Van Ness (1975) and Dean (1979) are at 25°C; Kang et al. (1992) report that K_{eq} is independent of temperature over the interval $75°C < T < 100°C$, since the heat of reaction is small. In view of this, the values of K_{eq} reported in Table 6 will not vary much over the normal boiling temperature range of the mixture. Barbosa and Doherty (1988b) showed that a quaternary reactive azeotrope of a saddle type would exist at the value of K_{eq} reported by Smith and Van Ness (1975), but not at the value given by Dean (1979).

In the previous examples, the systems were ternary and the mole fraction triangle reduced to a reactive edge. For quaternary reactive systems, the mole fraction space is tetrahedral and becomes planar in transformed composition variables. The two-dimensional analog of an inflexion singular point on a reactive edge is a saddle node on a face. Thus, starting points that possess the stability of saddle nodes are degenerate solutions to Eq. 4a or 4b.

Figure 15 illustrates the reactive residue curve maps in transformed composition variables, using ethyl acetate as a reference component. As K_{eq} approaches infinity (Figure 15a), the ternary azeotrope (point 1) is an unstable node (lowest boiling point) and the water–ethyl acetate azeotrope (point 2) is a saddle node. The point corresponding to the water–ethyl acetate azeotrope is degenerate since its stability is degenerate and it is therefore discarded. In contrast, the ternary azeotrope is a valid starting point because its stability is nondegenerate. This point along with the two nonreactive azeotropes and the four pure components form the set of valid starting points satisfying Eq. 4b. In Figure 15b, as K_{eq} approaches zero, it can be seen by inspection that the pure ethanol vertex is a saddle node. Therefore, the set of starting

Table 6. Values of K_{eq} for the Esterification of Acetic Acid with Ethanol

Reference	K_{eq}
Smith and Van Ness (1975)	0.25
Dean (1979)	10.2
Kang et al. (1992)	13.4

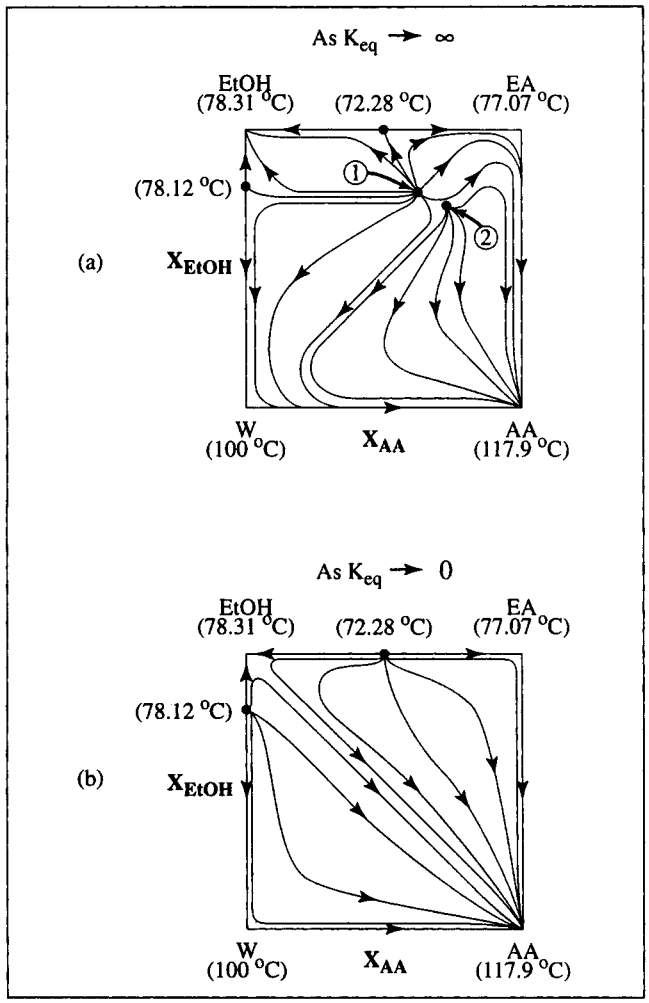

Figure 15. Reactive residue curve maps in transformed composition variables at different values of K_{eq}.

The solid circles signify the location of azeotropes. ① Minimum boiling ternary (EA–EtOH–W) azeotrope (70.23°C). ② Intermediate boiling binary (EA–W) azeotrope (70.38°C).

points consist of the other three pure-component vertices (EA, W, and AA) and the two azeotropes on the nonreactive edges.

From the bifurcation diagram shown in Figure 16, it is seen that as K_{eq} decreases from infinity, the minimum-boiling ternary azeotrope moves into the composition space, forming a minimum-boiling quaternary reaction azeotrope that merges with the nonreactive ethyl acetate–ethanol azeotrope at $K_{eq} \cong 12.5$. Barbosa and Doherty (1988b) calculated a residue curve map for $7.1 < K_{eq} < 8.2$ that showed no evidence of a reactive azeotrope. This is in agreement with the bifurcation diagram, which shows that the quaternary reactive azeotrope has already merged with the ethyl acetate–ethanol nonreactive azeotrope at this range of K_{eq}. Using the value of the reaction equilibrium constant calculated by Kang et al. (1992), Figure 16 predicts the appearance of a minimum-boiling quaternary reactive azeotrope near the nonreactive EA–EtOH azeotrope.

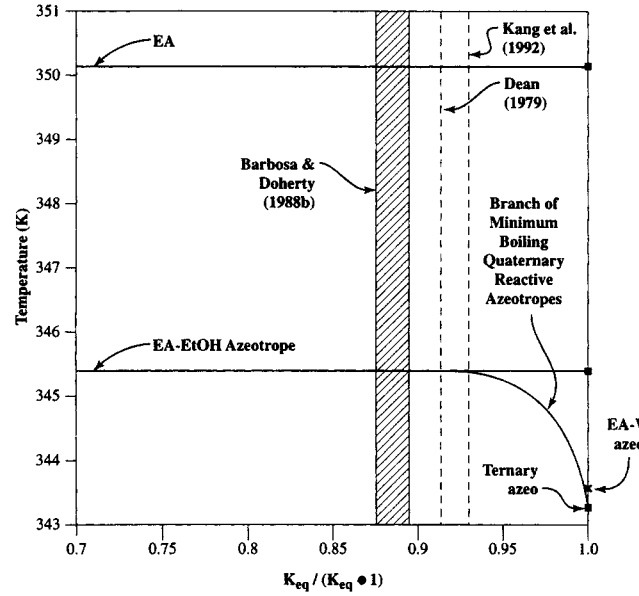

Figure 16. Portion of bifurcation diagram at high K_{eq} for ethyl acetate system.

The solid squares signify valid starting points, and the × signifies a degenerate solution of Eq. 4b and is not used as a starting point.

Barbosa and Doherty (1988b) also reported the presence of a quaternary saddle reactive azeotrope using the value of $K_{eq} = 0.25$ reported by Smith and Van Ness (1975). The bifurcation diagram, shown in Figure 17, confirms this finding and shows the evolution of this quaternary reactive azeotrope.

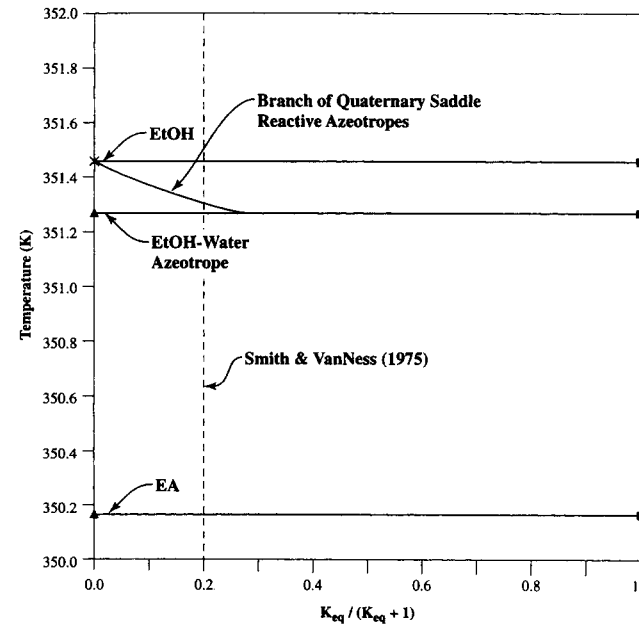

Figure 17. Portion of bifurcation diagram for the ethyl acetate system showing a quaternary reactive azeotrope at low K_{eq}.

The solid triangles and squares signify valid starting points, and × signifies a degenerate solution of Eq. 4a and is not used as a starting point.

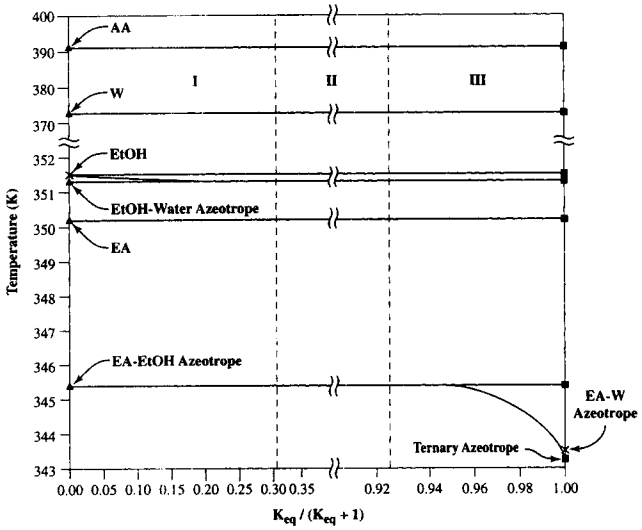

Figure 18. Composite of bifurcation diagram for three different regimes for the ethyl acetate system.

The solid triangles and squares signify valid starting points, and × signifies a degenerate solution of either Eq. 4a or 4b and is not used as a starting point.

It emerges from the pure ethanol vertex as K_{eq} increases from zero and moves through the composition tetrahedron until it asymptotically merges with the ethanol–water azeotrope at approximately $K_{eq} = 0.449$. The overall bifurcation diagram in Figure 18 shows three distinct regions exhibiting different residue curve maps for this system. In the first region, $K_{eq} < 0.449$, a quaternary saddle reactive azeotrope exists in the vicinity of the pure ethanol vertex. In region II, $0.449 < K_{eq} < 12.5$, there are no reactive azeotropes in the system. Above $K_{eq} = 12.5$, in region III, there emerges another quaternary reactive azeotrope (this time minimum-boiling) from the ethyl acetate–ethanol azeotrope that becomes the ternary nonreactive azeotrope in the limit as K_{eq} approaches infinity. This region has not been discovered previously in the literature. It is also worth noting the remarkable fact that each of the three literature values reported for K_{eq} fall into a *different* region of the phase behavior! More critical experiments are needed to determine which value of K_{eq} is correct.

Conclusions

Changes in the value of the reaction equilibrium constant affect the existence and location of reactive azeotropes. Reactive azeotropes, which arise from pure components and/or nonreactive azeotropes, may exist at all values of the reaction equilibrium constant or only over a small range. They can also move through a large portion of the composition diagram or may only exist within a certain region.

Starting with the definition of reactive azeotropy and the thermodynamic definition of the reaction equilibrium constant, a system of equations and a complete set of starting points can be easily determined with which to begin the arc-length continuation of the fixed-point branches. As seen from the examples, the bifurcation diagrams provide an efficient representation of the azeotropic behavior of reacting mixtures. These bifurcation diagrams clearly illustrate the existence, location, and the movement of reactive azeotropes as a function of the reaction equilibrium constant. In addition, regimes where the qualitative phase behavior of the system changes can be quickly identified.

The method outlined in this article offers several advantages for process design and development. It can rapidly screen classes of reactions for reactive azeotropy from knowledge of only pure components and nonreactive azeotropes. It can aid in process development by determining the existence and location of reactive azeotropes, and if the reactive distillation option is unfavorable, quickly determine if changes in system pressure can alter the reactive phase diagram sufficiently to yield feasible alternatives. Finally, when uncertainties exist in the value of the reaction equilibrium constant, a bifurcation diagram of the system illustrates whether small changes in K_{eq} will result in large qualitative changes in the phase diagram.

Acknowledgments

This research was supported by the sponsors of the University of Massachusetts Process Design and Control Center. We are grateful for the drafting services of Ms. Pamela Stephan.

Notation

a_i = activity of component i
C = number of components
T = temperature, K
x = liquid mole fraction
y = vapor mole fraction
ν_i = stoichiometric coefficient of component i
ν_T = sum of stoichiometric coefficients
X = transformed liquid composition variable
Y = transformed vapor composition variable

Subscript

i = component i

Literature Cited

Albert, M., I. Hahnenstein, H. Hasse, and G. Maurer, "Vapor–Liquid Equilibrium of Formaldehyde Mixtures," *AIChE J.*, **42**, 1741 (1996).

Barbosa, D., and M. F. Doherty, "Theory of Phase Diagrams and Azeotropic Conditions for Two-Phase Reactive Systems," *Proc. Roy. Soc. (London)*, **A413**, 443 (1987).

Barbosa, D., and M. F. Doherty, "The Influence of Equilibrium Chemical Reactions on Vapor-Liquid Phase Diagrams," *Chem. Eng. Sci.*, **43**, 529 (1988a).

Barbosa, D., and M. F. Doherty, "The Simple Distillation of Homogeneous Reactive Mixtures," *Chem. Eng. Sci.*, **43**, 541 (1988b).

Brandani, V., G. Di Giacomo, and P. U. Foscolo, "Isothermal Vapor-Liquid Equilibria for the Water-Formaldehyde System," *Ind. Eng. Chem. Proc. Des. Dev.*, **19**, 179 (1980).

Columbo, F., L. Cori, L. Dalloro, and P. Delogu, "Equilibrium Constant for the Methyl tert-Butyl Ether Liquid-Phase Synthesis by Use of UNIFAC," *Ind. Eng. Chem. Fundam.*, **22**, 219 (1983).

Dean, J. A., *Lange's Handbook of Chemistry*, 12th ed., McGraw-Hill, New York (1979).

Doedel, E., *AUTO: Software for Continuation and Bifurcation Problems in Ordinary Differential Equations*, Dept. of Mathematics, Cal. Inst. of Technol., Pasadena (1986).

Espinosa, J., P. Aguirre, and G. Perez, "Product Composition Regions of Single-Feed Reactive Distillation Columns," *Ind. Eng. Chem. Res.*, **34**, 853 (1995).

Fidkowski, Z. T., M. F. Malone, and M. F. Doherty, "Computing Azeotropes in Multicomponent Mixtures," *Comput. Chem. Eng.*, **17**, 1141 (1993).

Gmehling, J., and U. Onken, "Vapor-Liquid Equilibrium Data Collection, Aqueous-Organic Systems," *DECHEMA, Chem. Data. Ser.*, **1**(Part 1), 2; (Part 1a), 7; (Part 1b), 10 (1977).
Kang, Y., Y. Y. Lee, and W. K. Lee, "Vapor-Liquid Equilibria with Chemical Reaction Equilibrium—Systems Containing Acetic Acid, Ethyl Alcohol, Water and Ethyl Acetate," *J. Chem. Eng. Jpn.*, **25**, 649 (1992).
Keller, H. B., "Numerical Solution of Bifurcation and Nonlinear Eigenvalue Problems," *Applications of Bifurcation Theory*, P. H. Rabinowitz, ed., Academic Press, New York (1977).
Lee, L., and M. Kuo, "Phase and Reaction Equilibria of the Acetic Acid–Isopropanol–Isopropyl Acetate–Water System at 760 mm Hg," *Fluid Phase Equilibria*, **123**, 147 (1996).
Lin, W. J., J. D. Seader, and T. L. Wayburn, "Computing Multiple Solutions to Systems of Interlinked Separation Columns," *AIChE J.*, **33**, 886 (1987).
Maurer, G., "Vapor–Liquid Equilibrium of Formaldehyde and Water-Containing Multicomponent Mixtures," *AIChE J.*, **32**, 932 (1986).
Rehfinger, A., and U. Hoffmann, "Kinetics of Methyl Tertiary Butyl Ether Liquid Phase Synthesis Catalyzed by Ion Exchange Resin," *Chem. Eng. Sci.*, **45**, 1605 (1990).
Rhim, J. K., S. Y. Bae, and H. T. Lee, "Isothermal Vapor-Liquid Equilibrium Accompanied by Esterification: Ethanol-Formic Acid System," *Int. ChemEng.*, **25**, 551 (1985).
Seydel, R., *Practical Bifurcation and Stability Analysis— From Equilibrium to Chaos*, 2nd ed., Springer-Verlag, New York (1994).
Smith, J. M., and H. C. Van Ness, *Introduction to Chemical Engineering Thermodynamics*, 3rd ed., McGraw-Hill, New York (1975).
Ung, S., and M. F. Doherty, "Vapor-Liquid Phase Equilibrium in Systems with Multiple Chemical Reactions," *Chem. Eng. Sci.*, **50**, 23 (1995a).
Ung, S., and M. F. Doherty, "Necessary and Sufficient Conditions for Reactive Azeotropes in Multi-Reaction Mixtures," *AIChE J.*, **41**, 2383 (1995b).
Venimadhavan, G., G. Buzad, M. F. Doherty, and M. F. Malone, "Effect of Kinetics on Residue Curve Maps for Reactive Distillation," *AIChE J.*, **40**, 1814 (1994).
Venimadhavan, G., G. Buzad, M. F. Doherty, and M. F. Malone, "Correction," *AIChE J.*, **41**, 2613 (1995).

Appendix

In the first four examples, the vapor–liquid equilibrium equation used in this article is

$$Py_i = P_y^{\text{sat}} x_i \gamma_i$$

where

$$\ln P_i^{\text{sat}} = A_1 + A_2/(T + A_3) \qquad P = \text{Pa},\ T = \text{K} \quad \text{(A1)}$$

In Example 5, the dimerization of acetic acid in the vapor phase is accounted for by Eq. A2 from Barbosa and Doherty (1988a), where the dimerization correction factor (z) is calculated using Eq. A3:

$$Py_i z_i = P_i^{\text{sat}} x_i \gamma_i$$

where

$$\ln P_i^{\text{sat}} = A_1 + A_2/(T + A_3) \qquad P = \text{Pa},\ T = \text{K} \quad \text{(A2)}$$

$$z_A = \frac{1 + (1 + 4k_A P_A^{\text{sat}})^{1/2}}{1 + [1 + 4k_i P y_i (2 - y_i)]^{1/2}}$$

for an associating component

$$z_N = \frac{2\left\{1 - y_A + [1 + 4k_A P y_A (2 - y_A)]^{1/2}\right\}}{(2 - y_A)\left\{1 + [1 + 4k_A P y_A (2 - y_A)]^{1/2}\right\}} \quad \text{(A3)}$$

for nonassociating components where

$$\log_{10} k_A = D_1 + \frac{D_2}{T} \qquad k_A = \text{Pa}^{-1},\ T = \text{K}.$$

For calculating the activity coefficients in Eqs. A1 and A2, the form of the Wilson equation was taken from Gmehling and Onken (1977).

Manuscript received Dec. 16, 1996, and revision received May 23, 1997.